Proceedings of the 18th International Symposium on the
Packaging and Transportation of Radioactive Materials
PATRAM 2016
September 18-23, 2016, Kobe, Japan

Paper No. 2034

Flow characteristic inside a single basket includes a fuel assembly

Seung-Hwan Yu
Korea Atomic Energy Research Institute
Kyoung-sik Bang
KAERI
Woo-Seok Choi
KAERI
Ju-chan Lee
KAERI

Abstract

Flow characteristics inside a fuel basket containing a spent nuclear fuel assembly were analyzed. Since the geometry of a nuclear fuel assembly is very complicated, a porous media model and effective thermal conductivity were used to simplify the fuel assembly geometry. The permeability was calculated in three different ways. These included a theoretical approach using the friction force assuming laminar flow; a computational fluid dynamics (CFD) calculation using shear stress; and a CFD calculation using pressure drop. The results of the CFD calculations by shear stress and pressure drop showed good agreement. The result of the theoretical approach was 50% less than the CFD results. This was because the theoretical approach did not fully consider the flow resistance resulting from the complex geometry of the spacer grid and fuel rods

Introduction

A thermal evaluation must be included in the safety analysis report for a spent nuclear fuel transportation and storage system. The thermal behavior of the system depends on the flow of thermal fluid through it. However, the geometry of a nuclear fuel assembly is very complicated. To calculate the thermal-fluid flow characteristics for a system using the exact geometry of the fuel assembly requires a long time and a high performance computer cluster. In general, the porous media model and effective thermal conductivity are used to simply the fuel assembly.

In this study, computational modeling of a fuel assembly was used to investigate the thermal-fluid flow characteristics in a basket containing nuclear fuel. Three different methods of calculating the permeability were used and their results compared.

Modeling

The model for the calculation represented a spent nuclear fuel assembly loaded in a fuel basket. The canister was filled with helium. Helium flowed from the bottom to the top of the basket due to the natural convection produced by the decay heat of the spent nuclear fuel. The complex geometry of the nuclear fuel assembly induced a shear stress on the helium flow.

A model of the fuel assembly is shown in Fig. 1. The diameter of the fuel cladding was 9.5 mm. The spacer grids were located at regular intervals along the fuel rod except at the upper and lower end fittings. The flow resistance inside the basket was inversely proportional to the flow area. The lengths of the upper and lower end fittings were relatively short compared to the total height of the fuel assembly. The flow resistance generated by the upper and lower end fittings was negligible. Therefore, the upper and lower end fittings were not considered in the fuel assembly model.

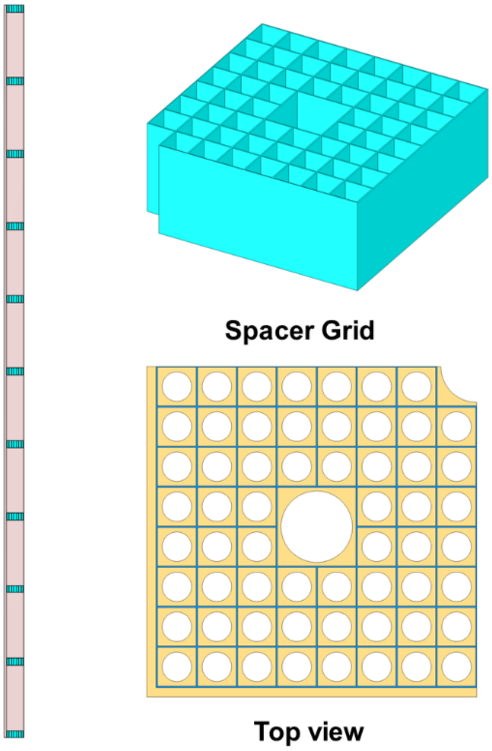

Figure 1 Modeling of a fuel assembly

Governing equations

For the numerical analysis, it was assumed that the flow was steady, laminar, and three-dimensional. The governing equations for the flow are as follows:

Continuity

$$\frac{\partial}{\partial x_i}\left(\rho u_i\right)=0$$

Momentum

$$\frac{\partial}{\partial x_i}\left(\rho u_i u_j\right)=-\frac{\partial p}{\partial x_i}+\frac{\partial \tau_{ij}}{\partial x_i}$$

where ρ is the density, u_i is the velocity component in the i direction, p is the static pressure, τ_{ij} is a stress tensor. The Ansys Fluent S/W was used for CFD calculation.

Boundary conditions and numerical procedure

Table 1 lists the imposed boundary conditions. The SIMPLE (Semi-Implicit Method for Pressure Linked Equations) algorithm was used to couple the velocity and pressure. For improved accuracy, a second-order upwind scheme was applied to the convective terms of the governing equations. The convergence criterion for all dependent variables was a relative error better than 10^{-5}.

Table 1 Boundary conditions for CFD

Wall	Boundary conditions
Bottom wall	Consistent velocity inlet
Top wall	Pressure outlet
Symmetric face	$\left.\frac{\partial u_{\mathrm{i}}}{\partial n}\right\|_{\text{sectional wall}} = 0$
Side face without symmetric face	$u_i = 0$

Results and discussions

Flow Characteristics inside the Basket

An upward natural convection occurred inside basket due to the decay heat of the spent nuclear fuel. Instead of considering the natural convection flow, the constant inlet velocity condition at the bottom inlet of the fuel assembly was used in the calculations. The range of velocities considered was 0.0–0.1 m/s. The walls of the fuel cladding, support rod, and grid spacers produced flow resistance. Planar sections at the different heights along the fuel assembly are shown in Fig. 2. Velocity contours for these planar sections are shown in Fig. 3. The flow velocity is relatively high at the planar sections that include a spacer grid due to the decreased cross sectional area at these points. The velocity distribution is almost even for the planar sections without a spacer grid.

Wall shear stress along the fuel rod is illustrated in Fig. 4. The highest wall shear stress occurred neat inlet area. When the flow developed, the high wall shear stress occurred at the beginning of the flow. Fully developed flow was broken by grid spacers. The flow developed again from the bottom of each grid spacer. Therefore, there were 11 peaks of wall shear stress.

Figure 5 shows the average static pressure and flow velocity as a function of height. As the height increases, the pressure decreases linearly. The average velocity increases and decreases with the same periodic pattern as the height. However, the mean value of the average velocity does not change. The linear pressure drop indicates that the flow resistance produced by the wall is constant along the fuel rod and the inertia resistance can be ignored. Therefore, only viscous flow resistance (permeability) is considered.

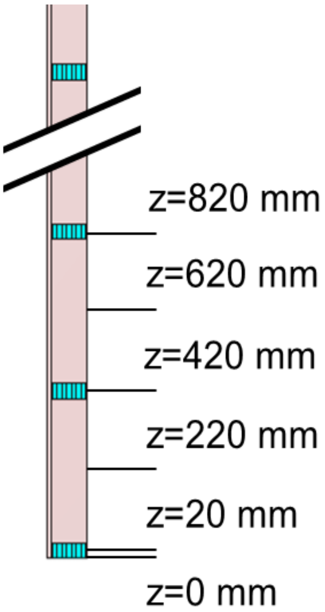

Figure 2 Location of planar section for velocity contour

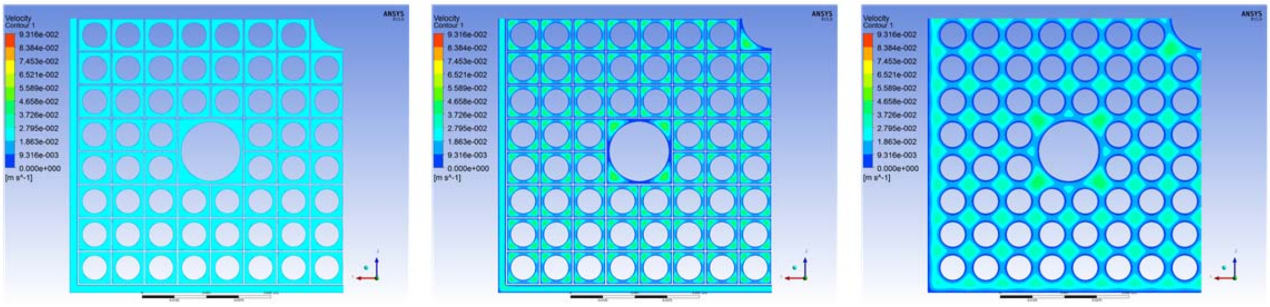

(a) z=0 mm (b) z=20 mm (c) z=220 mm

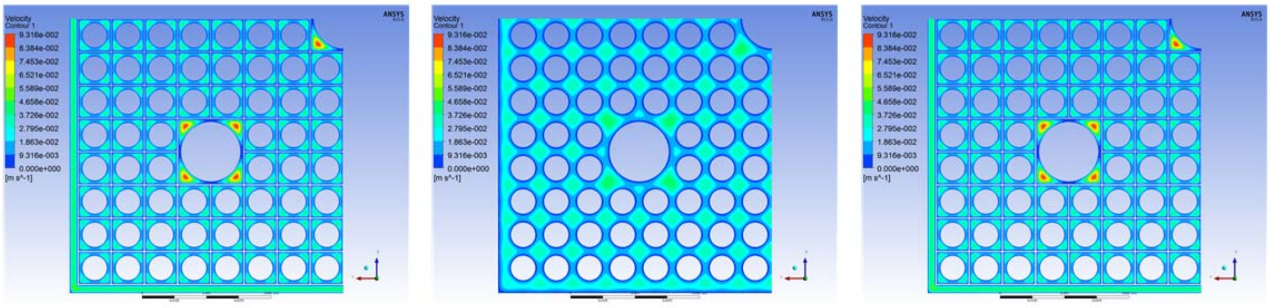

(d) z=420 mm (e) z=620 mm (f) z=820 mm

Figure 3 Velocity contours at the planar sections

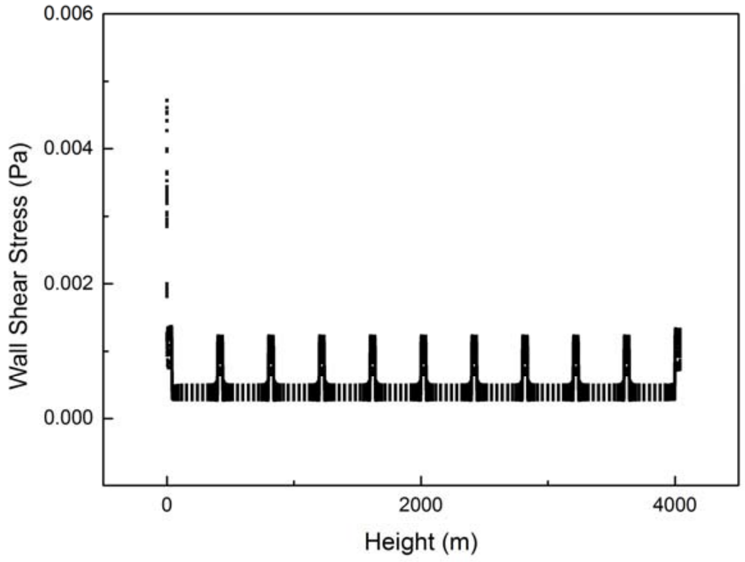

Figure 4 Wall shear stress as a function of height

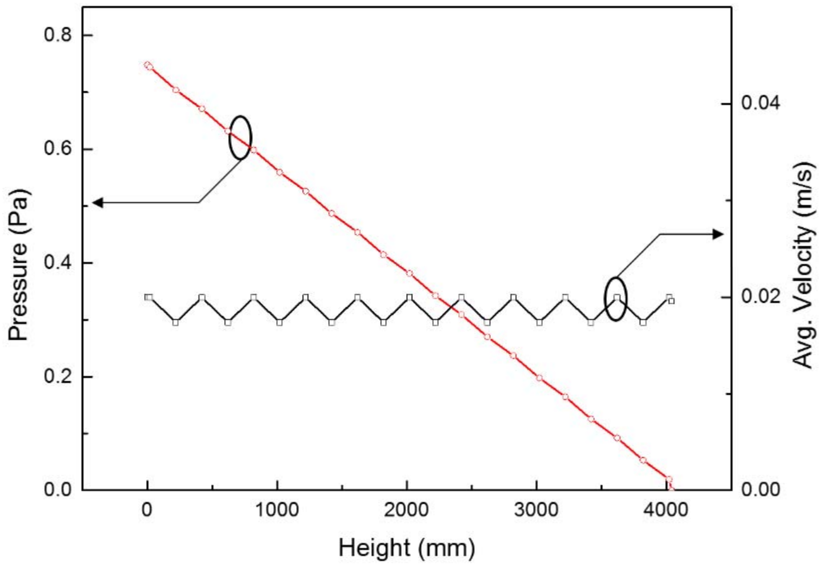

Figure 5 Average static pressure and velocity with according to height

Evaluation of Permeability

The permeability is calculated using three different methods. The first method is a theoretical approach using the friction factor. The second method is a CFD calculation using the wall shear stress. The third method is a CFD calculation using the pressure drop. The expressions for the permeability for the three methods are shown in Table 2.

Table 2 Permeability Calculation

Method	Friction factor	Wall shear stress	Pressure drop
Permeability	$\frac{32}{D_h^2}$	$\frac{4\tau_w}{\mu V D_h}$	$\frac{\Delta P}{L\mu V}$

The values in the calculation of the characteristic length are shown in Table 3. The total height of the grid spacer zones is 0.44 m and the total height of the fuel only zones is 3.6 m. If these heights are considered as the weighting factor, the characteristic length of the fuel assembly is 1.16×10^{-2} m. The permeability from the friction factor is 2.36×10^{5}.

Table 3 Calculation of characteristic length

	Grid spacer zone	Only fuel zone
Perimeter (mm)		
grid	1.30E+04	0.00E+00
fuel	7.04E+03	7.04E+03
support rod	3.92E+02	3.92E+02
basket	8.48E+02	8.48E+02
total	2.13E+04	8.28E+03
Area (mm^2)		
grid	3.31E+03	0.00E+00
fuel	1.67E+04	1.67E+04
support rod	2.45E+03	2.45E+03
basket	4.50E+04	4.50E+04
total	2.25E+04	2.58E+04
Characteristic length (mm)		
D_h	4.23E+00	1.25E+01

The permeability calculated from the wall shear stress is $4\tau_w/(\mu V D_h)$. The inlet velocity is set to each of the values 0.02, 0.04, 0.06, 0.08, 0.1 m/s, and the average wall shear stress is calculated at each velocity. The results are shown in Table 4. Calculations for the fuel and spacer grid zone were performed separately because the characteristic length of the fuel zone is not the same as that of the spacer grid zone. Although the inlet velocity changes, the average wall shear stress has the same value. The total average permeability from the wall shear stress is 5.17×10^{5}.

Table 4 Result of permeability by wall shear stress

V_{inlet} (m/s)	**Fuel zone (3.6 m)**			**Fuel and grid mix zone (0.44 m)**			D_{avg}
	V_{avg} (m/s)	τ_w **(Pa)**	**D**	**V_{avg} (m/s)**	τ_w **(Pa)**	**D**	
2.00E-02	1.75E-02	3.51E-04	3.24E+05	2.00E-02	8.81E-04	2.09E+06	5.16E+05
4.00E-02	3.50E-02	7.02E-04	3.24E+05	4.00E-02	1.77E-03	2.10E+06	5.17E+05
6.00E-02	5.24E-02	1.05E-03	3.24E+05	6.00E-02	2.65E-03	2.10E+06	5.18E+05
8.00E-02	7.00E-02	1.40E-03	3.24E+05	8.00E-02	3.54E-03	2.10E+06	5.18E+05
1.00E-01	8.75E-02	1.75E-03	3.24E+05	1.00E-01	4.43E-03	2.10E+06	5.18E+05

The permeability from the pressure drop is $\Delta P/\left(L\mu V\right)$. The pressure drop is the pressure difference between the inlet and outlet that are at the bottom and top of the fuel assembly, respectively. The results of the CFD calculation of the permeability from the pressures drop are shown in Table 5.

Table 5 Result of permeability by pressure drop

V_{inlet} (m/s)	**V_{avg} (m/s)**	ΔP **(Pa)**	**D**
0.02	1.77E-02	7.59E-01	5.33E+05
0.04	3.54E-02	1.52E+00	5.34E+05
0.06	5.32E-02	2.28E+00	5.34E+05
0.08	7.09E-02	3.04E+00	5.34E+05
0.1	8.86E-02	3.81E+00	5.34E+05

The calculated permeability using each of the three different methods described above are summarized in Table 6. The result for the friction factor method is 50% less than the results of the CFD calculations using wall shear stress and pressure drop. The assumption in the friction factor calculation that the flow is a laminar pipe flow could be the reason for the difference. The Darcy friction factor needs to be modified to calculate the exact shear stress of the fuel assembly.

Table 6 Summary of permeability calculation

Method	Friction factor	Wall shear stress	Pressure drop
Permeability	2.36E+05	5.17E+05	5.34E+05

Conclusions

The flow inside a fuel basket that contains a fuel assembly is analyzed using CFD. As the height of the fuel assembly increases, the average velocity demonstrates a repeated pattern and the static pressure decreases linearly. As a result, the porous media coefficient representing inertia resistance could be neglected. Three different methods were used to calculate the permeability and their results were compared. The friction factor method could be used to determine the approximate permeability without performing a CFD calculation. However, the permeability from the friction factor method is 50% less than the permeability from wall shear stress and pressure drop using CFD.

Acknowledgments

This work was supported by the Korean Ministry of Trade, Industry, and Energy (MOTIE) as a part of the Radioactive Waste Management Technology Development Project (201471020173B).

References

Ansys, Ansys 15.0 User guide(2015)

E. R. Lindgren and S.G. Durbin, “Laminar hydraulic analysis of a commercial pressurized water reactor fuel assembly”, NUREG /CR-7144(2013)

G. Zigh and J. Solis, “Computational fluid dynamics best practice guidelines for dry cask applications”, NUREG-2152(2013)